



Cite this: *RSC Adv.*, 2018, 8, 31261

# Detection of SO<sub>2</sub> derivatives using a new chalcocoumarin derivative in cationic micellar media: application to real samples†

Marisol Gómez,<sup>ID</sup>\*<sup>ab</sup> Margarita E. Aliaga,<sup>ID</sup><sup>a</sup> Verónica Arancibia,<sup>a</sup> Alexis Moya,<sup>a</sup> Camilo Segura,<sup>c</sup> Marco T. Nuñez,<sup>d</sup> Pabla Aguirre,<sup>d</sup> Edgar Nagles<sup>ID</sup><sup>e</sup> and Olimpo García-Beltrán<sup>ID</sup>\*<sup>e</sup>

A new probe (*E*)-7-(diethylamino)-3-(3-(thiophen-2-yl)acryloyl)-2*H*-chromen-2-one (ChC16) was synthesized and studied as a turn-on fluorescent probe, based on a Michael addition mechanism for sensing SO<sub>2</sub> derivatives, which is favored in the presence of cationic micellar media such as cetylpyridinium bromide (CPB). The probe showed high selectivity and sensitivity toward bisulfite over other anions and biothiols, including cysteine (Cys), homocysteine (Hcy) and glutathione (GSH), with a detection limit of 240 nM. Moreover, the probe showed great potential for its practical application in the detection of bisulfite in real samples, such as dry white wine, and in bioimaging.

Received 28th May 2018  
 Accepted 26th August 2018

DOI: 10.1039/c8ra04526g

[rsc.li/rsc-advances](http://rsc.li/rsc-advances)

## 1. Introduction

Sulfur dioxide (SO<sub>2</sub>) derivatives, such as sulfite (SO<sub>3</sub><sup>2-</sup>) and bisulfite (HSO<sub>3</sub><sup>-</sup>) ions, have been largely used as preservatives for many foodstuffs, drinks and medications.<sup>1</sup> However, it is well-known that all the SO<sub>2</sub> forms can potentially cause health problems. Specifically, it has been reported that elevated quantities of sulfite can cause asthma and allergic reactions in some people, including difficulty in breathing, urticaria and gastrointestinal discomfort.<sup>2-4</sup>

In this context, the Joint FAO/WHO Expert Committee on Food Additives has determined that an acceptable daily intake of sulfites should be lower than 0.7 mg kg<sup>-1</sup> of body weight.<sup>5</sup> Besides, since 1986 the FDA in the United States has demanded that any food or drink that contains a sulfite concentration bigger than 10 mg L<sup>-1</sup> (125 μM)<sup>6</sup> should be labelled. Therefore, the development of analytical methods that allow the detection and quantification of by-products of SO<sub>2</sub> have gained great interest.

At this time, there are several conventional methods for this purpose, such as iodometric titration,<sup>7</sup> chromatography,<sup>8,9</sup> electrochemical analysis<sup>10-12</sup> and flow injection analysis (FIA).<sup>13,14</sup> Nevertheless, the principal disadvantage of these methods is that the majority of them require sample pre-treatment and the use of multiple reagents. Furthermore, in some cases, the detection process is very low and depends on high-cost instruments.

By contrast, the current use of fluorescent probes as a detection technique has acquired great relevance due to their high sensitivity and accuracy. In this context, novelty fluorescent probes have been developed by the detection of SO<sub>2</sub> derivatives,<sup>15-19</sup> mainly based on reactions with HSO<sub>3</sub><sup>-</sup>/SO<sub>3</sub><sup>2-</sup>. Some examples reported in the literature are summarized in Table S1 (ESI†), and among this information we are interested in those that undergo a nucleophilic addition to “C=C” double bond, as a detection mechanism. Interestingly, Zhang *et al.* (2013)<sup>20</sup> reported promising studies in this area, using a cationic cetyltrimethylammonium bromide (CTAB) micelle, which created a hydrophobic microenvironment promoting the addition reaction from the sulfite to an activated olefin in aqueous solutions. Therefore, the selectivity and sensitivity of the probe improved considerably. More recently, we have reported new probes able to detect SO<sub>2</sub>-derivatives *via* a Michael-type addition reaction, which was also favored by micellar media.<sup>21</sup> In particular, we demonstrated that typical interferences, such as glutathione (GSH) and cysteine (Cys) were inhibited by the presence of the cationic micelles of cetylpyridinium bromide (CPB) and zwitterionic micelle of sulfobetaine (SB3-14) and the detection limits improved considerably. Thus, we take advantage of this fact and we are presenting in this study a new coumarin-chalcone derivative (*E*)-7-(diethylamino)-3-(3-(thiophen-2-yl)acryloyl)-2*H*-

<sup>a</sup>Facultad de Química, Pontificia Universidad Católica de Chile, Vicuña Mackenna 4860, Santiago, 7820436, Chile

<sup>b</sup>Escuela de Obstetricia y Puericultura and Centro Integrativo de Biología y Química Aplicada (CIBQA), Universidad Bernardo O'Higgins, General Gana 1702, Santiago, 8370993, Chile

<sup>c</sup>Department of Chemistry, Faculty of Sciences, Universidad de Chile, Santiago 7800024, Chile

<sup>d</sup>Biology Department, Faculty of Sciences, Universidad de Chile, Santiago 7800024, Chile

<sup>e</sup>Facultad de Ciencias Naturales y Matemáticas, Universidad de Ibagué, Carrera 22 Calle 67, Ibagué 730001, Colombia. E-mail: jose.garcia@unibague.edu.co

† Electronic supplementary information (ESI) available. See DOI: 10.1039/c8ra04526g



chromen-2-one (**ChC16**). The latter would undergo a nucleophilic addition reaction of  $\text{SO}_2$ -derivatives to its "C=C" double bond, favored by the use of a cationic micelle.

## 2. Results and discussion

### 2.1 Synthesis and characterization of probe (**ChC16**)

We describe here a new probe **ChC16** (Scheme 1), which was designed considering a diethylaminocoumarin unit, as the fluorophore,<sup>5</sup> bound *via* a double bond (C=C) with a thiophene fragment. The bond (C=C) would be responsible for the recognition of  $\text{SO}_2$ -derivatives *via* a nucleophilic addition reaction. The latter based on previous studies, which demonstrated that other chalcone-coumarin derivatives were able to act as fluorescent sensors for biothiols based on Michael addition.<sup>22,23</sup> Regarding the thiophene fragment, it is considered as a good moiety for Michael acceptor. In fact, studies demonstrated that 2-(2-nitrovinyl)thiophene is only a little less reactive than the well-known Michael acceptor *trans*  $\beta$ -nitrostyrene.<sup>24</sup>

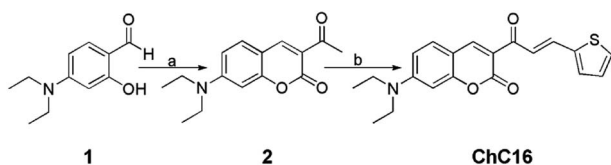
The new compound **ChC16** was synthesized in two steps, as shown in Scheme 1. Firstly, 4-diethylaminosalicylaldehyde (**1**) was condensed with ethyl acetoacetate (Knoevenagel) and cyclized obtaining the compound 3-acetyl-7-(diethylamino)-2H-chromen-2-one (**2**).<sup>25</sup> Finally, **ChC16** was synthesized by adaptations of a literature procedure<sup>26</sup> and characterized by <sup>1</sup>H-NMR, <sup>13</sup>C-NMR and HRMS (S1–S3; ESI<sup>+</sup>).

### 2.2 Absorption and emission properties of the probe (**ChC16**) in a micellar media of CPB

The absorption and emission properties of the **ChC16** derivative at neutral conditions, 20 mM Britton–Robinson (BR) buffer (pH  $\approx$  7) containing 1% (v/v) DMSO were assessed. Probe **ChC16** exhibits an absorption band with a maximum at 450 nm (Fig. S4; ESI<sup>+</sup>), a molar absorptivity ( $\epsilon_{450}$ ) of 23 888 L mol<sup>-1</sup> cm<sup>-1</sup> (Fig. S5; ESI<sup>+</sup>) and a characteristic emission  $\sim$ 500 nm. In the presence of the micelle CPB, the absorption band associated with **ChC16** is well defined and centered at 460 nm. Regarding the intensity of fluorescence emission (centered on 500 nm), it considerably increased by CPB effect. As shown in Table 1, the quantum yields were determined to be 0.169 and 0.349 for **ChC16** in absence and presence of CPB, respectively.

### 2.3 Effect of pH on the fluorescence response of the probe **ChC16** toward $\text{SO}_2$ -derivatives

To ensure the optimal conditions to efficiently detect  $\text{SO}_2$  derivatives ( $\text{HSO}_3^-/\text{SO}_3^{2-}$ ) with the tested derivative (**ChC16**),



**Scheme 1** Synthetic route for probe **ChC16**. Reagents and conditions: (a) ethyl acetoacetate, piperidine, AcOH, EtOH, reflux, 6 h; (b) 2-thiophenecarboxaldehyde, DCM, reflux, 12 h.

**Table 1** Photophysical parameters of the tested fluorescent **ChC16** in the absence and presence of CPB and  $\text{Na}_2\text{SO}_3$  in aqueous solution

[CPB] (mM)	$[\text{Na}_2\text{SO}_3]$ ( $\mu\text{M}$ )	$\lambda_{\text{Abs}}$ (nm)	$\lambda_{\text{Emi}}$ (nm)	$\epsilon$ ( $\text{M}^{-1} \text{cm}^{-1}$ )	$\phi$
—	—	450	500	23 888	0.169
1.5	—	460	490	36 034	0.349
—	500	450	500	28 434	0.381
1.5	500	460	490	31 546	0.893

we evaluated the changes in the fluorescence intensity associated with it. The latter was carried out in the presence of  $\text{Na}_2\text{SO}_3$ , at different pH values. As it can be seen in Fig. 1, the fluorescence response of probe **ChC16** alone was almost pH insensitive, whereas upon the interaction with  $\text{Na}_2\text{SO}_3$  important changes were observed depending on the pH values, showing a high fluorescence response from pH 6 to 9. In fact, a pH value of 7 was found to be appropriate for the bisulfite/sulfite detection by probe **ChC16**. The latter suggests that this probe can successfully react with  $\text{HSO}_3^-/\text{SO}_3^{2-}$  and allow for them to be detected in physiological conditions.

Considering these results, we assessed the effect of adding increasing concentrations of  $\text{Na}_2\text{SO}_3$  on the intensity of the emission band of **ChC16** at 490 nm, in the presence of CPB. As shown in Fig. 2(A), the emission band peak of probe in the presence of different concentrations of  $\text{Na}_2\text{SO}_3$  (0–10 equivalent) gradually increased. The intensity of emission changed from 110 to 700 arbitrary units (see quantum yields in Table 1) and the reaction could be completed in 15 min. As a result, a good linear relationship between them was observed; thus, based on this linearity (Fig. 2(B)), the detection limit was determined to be 240 nM (S/N = 3). This value was lower to those reported in the literature for other probes for sulfite in the absence of the micellar medium.<sup>21,27</sup>

Regarding the stability of the method, this was mentioned in the Experimental section. The relative standard deviation (RSD) of the detection associated with the probe in the presence of the cationic micelle was 2%. It is important to mention that lesser values to 5% are accepted.<sup>28</sup>

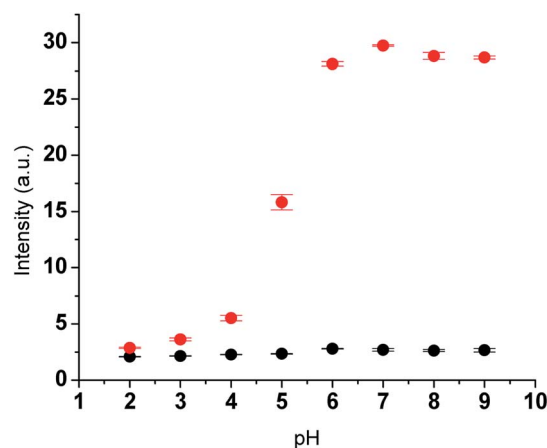


**Fig. 1** Effect of pH on the fluorescence intensity of the **ChC16** (5  $\mu\text{M}$ ) alone (●) and after its reaction with  $\text{Na}_2\text{SO}_3$  (10  $\mu\text{M}$ ) (●) at 25 °C after 120 min of reaction. Emission at 485 nm was measured.  $\lambda_{\text{ex}}$  = 450 nm. Slits 5 nm.



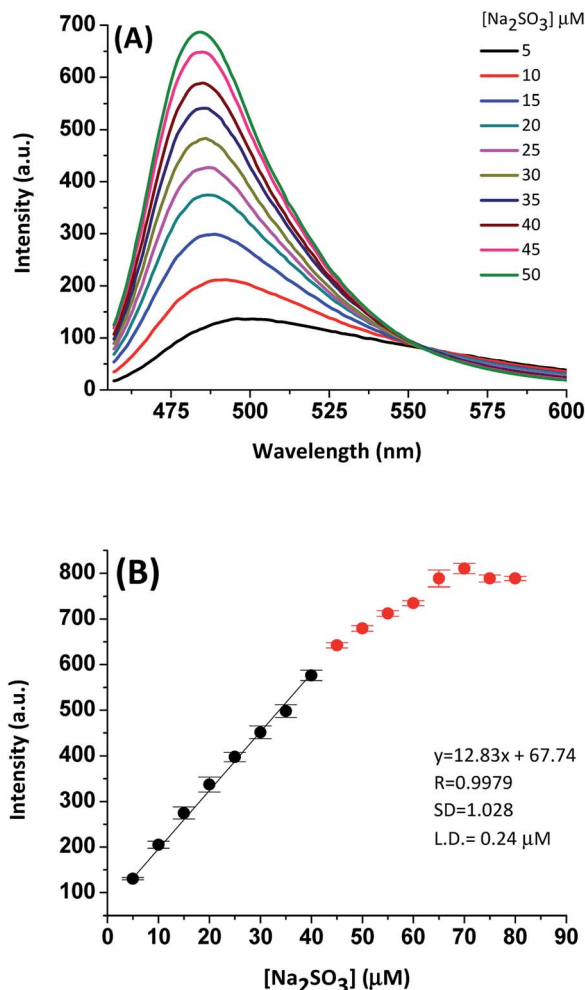


Fig. 2 (A) Fluorescence spectra of ChC16 (10  $\mu\text{M}$ ) upon the addition of increasing concentration of  $\text{Na}_2\text{SO}_3$  from 5 to 50  $\mu\text{M}$  in Britton–Robinson (BR) buffer solution (20 mM, pH 7, 1% DMSO) in the presence of 1.5 mM of CPB;  $\lambda_{\text{ex}} = 450$  nm. (B) Changes in fluorescence intensity of ChC16 at 480 nm upon the gradual addition of  $\text{Na}_2\text{SO}_3$  from 5 to 80  $\mu\text{M}$ ;  $\lambda_{\text{ex}} = 485$  nm; slits, 5 nm.

#### 2.4 Selectivity and competition studies of the probe ChC16 toward $\text{SO}_2$ -derivatives over other analytes

With the aim to evaluate the selectivity of the tested probe (ChC16) toward  $\text{SO}_2$  derivatives, we investigate its fluorescence response to typical interfering anions such as  $\text{F}^-$ ;  $\text{Cl}^-$ ;  $\text{Br}^-$ ;  $\text{I}^-$ ;  $\text{NO}_3^-$ ;  $\text{NO}_2^-$ ;  $\text{SO}_4^{2-}$ ;  $\text{SCN}^-$ ;  $\text{S}_2\text{O}_3^{2-}$ ;  $\text{S}_2\text{O}_4^{2-}$ ;  $\text{S}^{2-}$ ;  $\text{CH}_3\text{COO}^-$ ;  $\text{HCO}_3^-$ ;  $\text{H}_2\text{PO}_4^-$  and biothiols (*i.e.* cysteine (Cys) and glutathione (GSH)). As illustrated in Fig. 3, no significant variations in the fluorescence emission associated to the probe were observed, for most of these anions, even in the presence of 10 eq. of the anions mentioned above. Except a slight change in the probe intensity was observed when the biothiol (GSH) was assessed.

Furthermore, a competitive analysis of the different tested anions with  $\text{HSO}_3^-/\text{SO}_3^{2-}$  was conducted. As shown in Fig. 4, after adding  $\text{SO}_2$  derivatives into the solution containing other anions, no significant variation in fluorescence intensity associated with ChC16 was found. It can be noted that all the tested

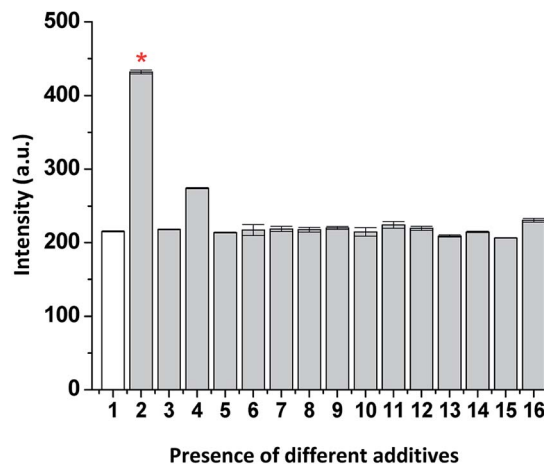


Fig. 3 Fluorescence intensities ( $\lambda_{\text{ex}} = 450$  nm) of ChC16 (10  $\mu\text{M}$ ) upon addition of various anions (100  $\mu\text{M}$ ) in the presence of 1.5 mM of CPB. White bar represents: ChC16 alone (1) and grey bars represent:  $\text{NO}^-$  + anions (2)  $\text{HSO}_3^-$  (\*); (3) cysteine; (4) glutathione; (5)  $\text{F}^-$ ; (6)  $\text{Cl}^-$ ; (7)  $\text{Br}^-$ ; (8)  $\text{I}^-$ ; (9)  $\text{CH}_3\text{COO}^-$ ; (10)  $\text{NO}_2^-$ ; (11)  $\text{NO}_3^-$ ; (12)  $\text{HCO}_3^-$ ; (13)  $\text{H}_2\text{PO}_4^-$ ; (14)  $\text{SO}_4^{2-}$ ; (15)  $\text{S}_2\text{O}_3^{2-}$ ; (16)  $\text{S}^{2-}$ . Slits 5 nm. The symbol (\*) represents the analyte of interest.

anions have no interference with the fluorescence response of ChC16 toward  $\text{HSO}_3^-/\text{SO}_3^{2-}$ , thereby indicating its high selectivity.

#### 2.5 Sensing mechanism of the probe ChC16 toward $\text{SO}_2$ -derivatives

Considering that both  $\text{HSO}_3^-/\text{SO}_3^{2-}$  can be acting as nucleophiles, we proposed that their addition to the double bond ( $\text{C}=\text{C}$ ) of the probe could be responsible for the change in the fluorescence emission.

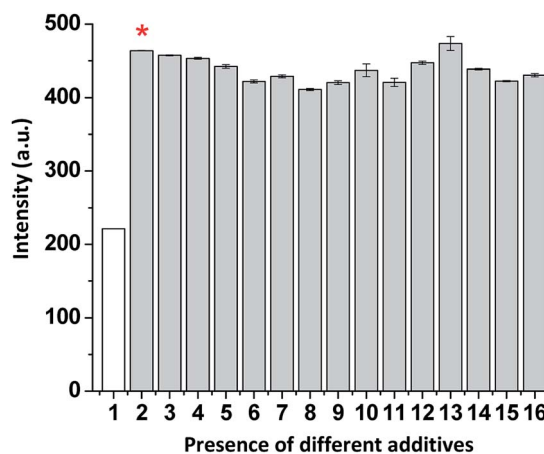


Fig. 4 Fluorescence intensities ( $\lambda_{\text{ex}} = 450$  nm) of ChC16 (10  $\mu\text{M}$ ) upon addition of various anions (100  $\mu\text{M}$ ) in the presence of 1.5 mM of CPB. White bar represents: ChC16 alone (1) and grey bars represent: ChC16 in the presence of  $\text{HSO}_3^-$  (2) and other anions; (3) cysteine; (4) glutathione; (5)  $\text{F}^-$ ; (6)  $\text{Cl}^-$ ; (7)  $\text{Br}^-$ ; (8)  $\text{I}^-$ ; (9)  $\text{CH}_3\text{COO}^-$ ; (10)  $\text{NO}_2^-$ ; (11)  $\text{NO}_3^-$ ; (12)  $\text{HCO}_3^-$ ; (13)  $\text{H}_2\text{PO}_4^-$ ; (14)  $\text{SO}_4^{2-}$ ; (15)  $\text{S}_2\text{O}_3^{2-}$ ; (16)  $\text{S}^{2-}$ . Slits 5 nm. The symbol (\*) represents the analyte of interest.



In order to confirm the proposed mechanism for the response of the probe after its interaction with  $\text{HSO}_3^-/\text{SO}_3^{2-}$ , first we carried out experiments using high resolution mass spectroscopy (HRMS-ESI).

Results from the HRMS-ESI (Fig S6; ESI<sup>†</sup>) show a major ion peak found at  $m/z$  435.1598 which is nearly identical to the theoretical molecular mass of the **ChC16**-bisulfite adduct ( $[\text{ChC16-H}]^+$  calcd 435.0858). These data strongly support the 1 : 1 adduct formation of probe **ChC16** mainly with bisulfite (**ChC16-SO<sub>3</sub>H**).

Subsequently, we assessed the interaction mode between **ChC16** and bisulfite using <sup>1</sup>H-NMR spectroscopy. As shown in Fig. 5A, the spectrum of **ChC16** in the absence of  $\text{Na}_2\text{SO}_3$  depicts two important signals at 7.93 and 7.75 ppm, which could be attributed to the vinylic protons H<sub>b</sub> and H<sub>a</sub>, respectively. Upon the addition of  $\text{Na}_2\text{SO}_3$  to a solution containing the probe, the resulting spectrum presents a new signal that appears at 5.08 ppm (Fig. 5(B)), which is attributed to the proton H<sub>b</sub> that was upfield shifted. These data suggest that the reaction between bisulfite and **ChC16** is a Michael addition in the β-carbon of the ketone α,β-unsaturated. This result is consistent with the formation of the **ChC16-SO<sub>3</sub>H** adduct.

## 2.6 Validation and application to real samples

In order to demonstrate the applicability of the tested probe, compound **ChC16** was assessed to detect  $\text{HSO}_3^-$  in real samples. In the first case, the real sample included white wines, which were analyzed using probe **ChC16** in the presence of CPB as a fluorometric method and a reported method to determine the total sulfite concentration.<sup>29</sup> As shown in Table 2, the obtained results using these two detection methods for bisulfite perfectly fit (error range 4–9%). Thus, these results suggest that probe **ChC16**, in the presence of a cationic micelle as CPB, can be used for quantitative detection of  $\text{HSO}_3^-$  in a real sample.

Furthermore, bearing in mind evidence on the production of sulfur dioxide in cytosols and mitochondria of cells<sup>30</sup> we also assessed whether the probe can determine  $\text{SO}_2$  derivatives in biological systems. As shown in Fig. 6(A), when SH-SY5Y

**Table 2** Determination of bisulfite concentration in real samples, see details in Experimental section

Sample	Fluorometric method using ChC16 + CPB	AOAC Official Method <sup>29</sup>
Wine 1	104.7 [mg L <sup>-1</sup> ]	100.3 [mg L <sup>-1</sup> ]
Wine 2	115.3 [mg L <sup>-1</sup> ]	119.6 [mg L <sup>-1</sup> ]

neuroblastoma cells were incubated with **ChC16** (5 μM) for about 20 min at 37 °C, a low intracellular fluorescence was observed, with cytoplasmic accumulation. After treatment of cells with  $\text{Na}_2\text{SO}_3$  (30 μM) for an additional 45 min at 37 °C, a slight increase in the fluorescence signal was detected (not shown).

However, other experiments demonstrated that, when SH-SY5Y cells were incubated with **ChC16** (5 μM) in the presence of the cationic micelle CPB (1 mM) and  $\text{Na}_2\text{SO}_3$  for an additional 15 min at 37 °C, a large increase in fluorescent intensity could be observed. Thus, demonstrating that the compound **ChC16** acts as a probe “turn on” induced by the mixture CPB- $\text{SO}_2$  derivatives. Finally, it is important to mention that the **ChC16** compound has a diethylamino group at the C-7 of the coumarin and this group have shown affinity for the cell membrane.<sup>25</sup> However, in this study it was observed that the compound have no affinity by cell membrane. Moreover, an accumulation in cytoplasmic structures was observed.

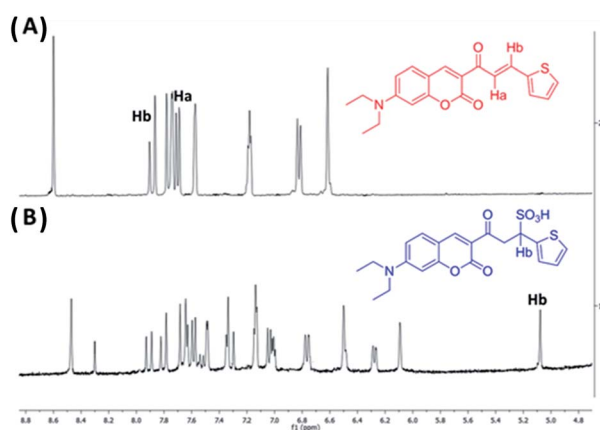


**Fig. 5** <sup>1</sup>H-NMR partial of **ChC16** in the absence (A) and in the presence (B) of  $\text{Na}_2\text{SO}_3$  (10 eq.), solvent used  $\text{DMSO-d}_6$  :  $\text{D}_2\text{O}$  (4 : 1).

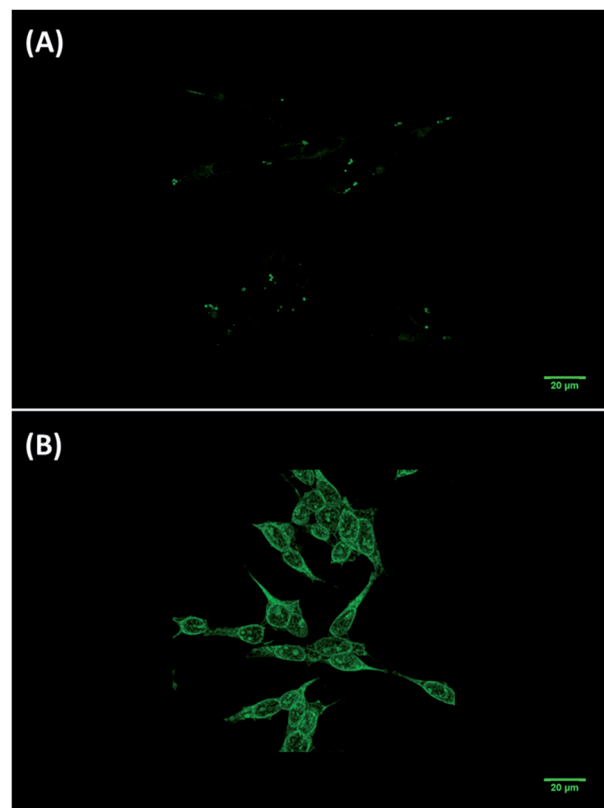


**Fig. 6** Fluorescence images of SH-SY5Y cells. (A) Cells were incubated with probe **ChC16** (5 μM) for 20 min; (B) image of cells after subsequent treatment with CPB (1 mM) and  $\text{Na}_2\text{SO}_3$  (30 μM) for 15 min.



### 3. Conclusions

In this work, we synthesized and characterized a new chalcocoumarin derivative and we assessed its photo-physical behavior as a sensor for SO<sub>2</sub> derivatives. We found that this probe, in the presence of a cationic micellar medium, displays a high selectivity for sulfite over the other typical interferents (biothiols) with a detection limit next to 10<sup>-9</sup> M. Finally, we were able to carry out experiments in real samples of white wine and cell imaging to visualize bisulfite by the proposed fluorometric method, using **ChC16** in a micellar cationic media.

### 4. Experimental

#### 4.1 Synthetic procedures

**4.1.1 Synthesis of (*E*)-3-(3-(1*H*-pyrrol-2-yl)acryloyl)-7-(diethylamino)-2*H*-chromen-2-one.** 4-Diethylaminosalicylaldehyde (**1**) (2.0 g, 10.4 mmol), ethyl acetoacetate (2.6 g, 20 mmol), piperidine (0.5 mL) and one drop of AcOH, were combined in absolute EtOH (60 mL) and refluxed for 6 h and cyclized in a single step to afford obtaining the compound 3-acetyl-7-(diethylamino)-2*H*-chromen-2-one (**2**). Subsequently, compound **2** (0.5 g, 1.9 mmol) and 2-thiophenecarboxaldehyde (0.2 g, 1.9 mmol) were dissolved in 10 mL of EtOH and 0.3 mL of piperidine were added to this solution. The mixture was kept at reflux temperature for 14 h. The solution was concentrated under reduced pressure. The solid was finally purified by CC on silica gel eluting with DCM : AcOEt 15 : 1. The product obtained is a yellow solid (0.478 g, 1.35 mmol) in 71.0% yield. <sup>1</sup>H-NMR (400 MHz, DMSO-*d*<sub>6</sub>) δ 8.57 (s, 1H), 7.93 (d, 1H, *J* = 20 Hz, Ar-CH, H3'), 7.75 (d, 1H, *J* = 20 Hz, CO-CH=, H2'), 7.73 (s, 1H, Ar-H, H4), 7.68 (d, 1H, *J* = 12 Hz, Ar-H, H4''), 7.56 (d, 1H, *J* = 12 Hz, Ar-H, H6, H8), 7.17 (t, 1H, *J* = 4.0 Hz, Ar-H, H6), 6.80 (d, 1H, *J* = 4.0 Hz, Ar-H, H6), 6.59 (s, 1H), 3.50 (dd, 4H, *J* = 8.0, -CH<sub>2</sub>-), 1.15 (s, 6H, *J* = 8.0, -CH<sub>3</sub>). <sup>13</sup>C-NMR (100 MHz, DMSO-*d*<sub>6</sub>) 12.8, 44.9, 96.3, 108.4, 110.7, 115.6, 124.0, 129.2, 130.2, 133.0, 133.4, 135.5, 140.7, 148.9, 153.3, 158.7, 160.5, 185.3. The *m/z* observed value was 354.1148 positive mode, and the calculated value for C<sub>20</sub>H<sub>19</sub>NO<sub>3</sub>S was 353.1085 (Fig. S3†).

#### 4.2 Materials and methods

Solvents and reagents utilized were Sigma-Aldrich. All solutions employed in this study were prepared in Britton-Robinson (BR) buffer solution (20 mM, pH = 7) and the reagents utilized were Suprapur®. The stock dissolution of the probe was conducted in DMSO. Absorption and fluorescence spectra were obtained HP-8453 diode array spectrophotometer and Cary Eclipse fluorescence spectrophotometer, respectively.

**4.2.1 High-resolution mass spectrometry (HRMS-ESI) studies.** High-resolution mass spectra (HRMS-ESI) were extracted from high resolution mass spectrometer Exactive™ Plus Orbitrap, ThermoFisher Scientific. The analysis for the reaction products was performed with the following scan parameters: resolution 140.000; AGC target 1e6; inject time 200. HESI source was heath gas flow 8; auxiliary gas flow rate 3; sweep gas flow rate 0; capillary temperature 250 °C, S-lens RF 100; heater temperature 100 °C, at mode positive with spray voltage 2.8 kV.

**4.2.2 Nuclear magnetic resonance (NMR) studies.** <sup>1</sup>H and <sup>13</sup>C NMR spectra were obtained at 25 °C on a Bruker Avance 400 MHz spectrometer using TMS as an internal standard. The NMR spectra were processed with MestreNova software v9.0. All solutions were prepared by mixing appropriate volumes of stock solutions of **ChC16** in DMSO-*d*<sub>6</sub> and D<sub>2</sub>O.

**4.2.3 Determining the quantum yield of emission.** Fluorescence quantum yields **ChC16** were measured using a solution of quinine sulfate in 0.5 M H<sub>2</sub>SO<sub>4</sub> as standard ( $\Phi_s = 0.546$ )<sup>31</sup> for probe. All values were corrected taking into account the solvent refraction index. Quantum yields were calculated using eqn (1),<sup>31</sup> where the subscripts x and s denote sample and standard, respectively,  $\Phi$  is the quantum yield,  $\eta$  is the refractive index, and Grad is the slope from the plot of integrated fluorescence intensity vs. absorbance.

$$\Phi_x = \Phi_s \left( \frac{\text{Grad}_x}{\text{Grad}_s} \right) \left( \frac{\eta_x^2}{\eta_s^2} \right) \quad (1)$$

**4.2.4 Reproducibility.** The stability of the method was determined into measuring the intensity of fluorescence in the wavelength of the peak of emission in the presence of CPB for 30 successive measures each 5 minutes. The shrunk data were examined in the software Origin 8.0.

**4.2.5 Detection limit.** The detection limit (LOD) was calculated based on fluorescence of the successive additions of the probe. To determine the S/N ratio, the emission intensity of each probe with Na<sub>2</sub>SO<sub>3</sub> was measured for three times and the standard deviation of calibration curve was determined. The LOD was calculated from  $\text{LOD}_{(y)} = a + 3\sigma_{x/y}$  and  $\text{LOD}_{(y)} = a + b\text{LOD}$ , where *a* is the intercept,  $\sigma_{x/y}$  is the random error in *x* and *y*, and *b* is the slope of the plot of fluorescence intensity versus sample concentration.<sup>21</sup> In addition,  $\text{LOD} = \text{LOD}_{(x)} = 3\sigma_{x/y}/b$ , assuming that errors principally occur in the *y*-direction.

**4.2.6 Preparation of real samples.** The studied samples were commercial white wines. For this, 30 mL of a newly opened wine bottle was taken and 5 g of activated carbon was added. After 30 min, the sample was filtered with syringe filters 0.45 micron to remove carbon. Subsequently each sample was added to the fluorescence cuvette, it contained Britton-Robinson (BR) buffer solution (20 mM, pH 7, 1% DMSO) in the presence of 1.5 mM of CPB. Subsequently, successive additions of Na<sub>2</sub>SO<sub>3</sub> were carried out and using the standard addition method. The concentration of the sample was determined.

**4.2.7 Cell culture and fluorescence imaging.** SH-SY5Y neuroblastoma cell lines (CRL-2266, American Type Culture Collection, Rockville, MD) were cultured in MEM/F12 medium supplemented with 10% fetal bovine serum (FBS), non-essential amino acids, antibiotic-antimycotic mixture, and 20 mM HEPES buffer, pH 7.4. The medium was replaced every 2 days. Cells were exposed and incubated with, **ChC16** (5 μM, 20 min) and the basal fluorescence of the probe was measured. In other cases, adding one mix incubated with **ChC16** (5 μM) in the presence of the cationic micelle CPB (1 mM), Na<sub>2</sub>SO<sub>3</sub> (30 μM) for about 15 min, and washed with HBSS with calcium and magnesium salts, after that the fluorescence was determined.



The fluorescence change was measured and observed using a confocal microscopy at 63× amplification. Confocal microscopy Zeiss 710.

## Conflicts of interest

There are no conflicts to declare.

## Acknowledgements

This work was supported by FONDECYT postdoc grant #3150196, FONDECYT grants #1170753 and #11170701, and by COLCIENCIAS Grants #130774559056 Colombia.

## References

- 1 R. F. McFeeters and A. O. Barish, *J. Agric. Food Chem.*, 2003, **51**, 1513–1517.
- 2 C. Wang, S. Feng, L. Wu, S. Yan, C. Zhong, P. Guo, R. Huang, X. Weng and X. Zhou, *Sens. Actuators, B*, 2014, **190**, 792–799.
- 3 X. Ma, C. Liu, Q. Shan, G. Wei, D. Wei and Y. Du, *Sens. Actuators, B*, 2013, **188**, 1196–1200.
- 4 S. L. Bahna and J. G. Burkhardt, *Allergy Asthma Proc.*, 2018, **39**, 3–8.
- 5 M.-Y. Wu, T. He, K. Li, M.-B. Wu, Z. Huang and X.-Q. Yu, *Analyst*, 2013, **138**, 3018–3025.
- 6 U.S. Food and Drug Administration, 1986, **51**, 25012–25020.
- 7 J. M. Vahl and J. E. Converse, *J. Assoc. Off. Anal. Chem.*, 1980, **63**, 194–199.
- 8 D. R. Migneault, *Anal. Chem.*, 1989, **61**, 273–275.
- 9 Z. Zhong, G. Li, B. Zhu, Z. Luo, L. Huang and X. Wu, *Food Chem.*, 2012, **131**, 1044–1050.
- 10 Ü. T. Yilmaz and G. Somer, *Anal. Chim. Acta*, 2007, **603**, 30–35.
- 11 A. Isaac, J. Davis, C. Livingstone, A. J. Wain and R. G. Compton, *TrAC, Trends Anal. Chem.*, 2006, **25**, 589–598.
- 12 M. H. Pournaghi-Azar, M. Hydarpour and H. Dastangoo, *Anal. Chim. Acta*, 2003, **497**, 133–141.
- 13 C. Ruiz-Capillas and F. Jimenez-Colmenero, *Food Addit. Contam., Part A*, 2008, **25**, 1167–1178.
- 14 S. S. M. Hassan, M. S. A. Hamza and A. H. K. Mohamed, *Anal. Chim. Acta*, 2006, **570**, 232–239.
- 15 J. Chao, X. Wang, Y. Liu, Y. Zhang, F. Huo, C. Yin, M. Zhao, J. Sun and M. Xu, *Sens. Actuators, B*, 2018, **272**, 195–202.
- 16 J. Chao, H. Wang, Y. Zhang, C. Yin, F. Huo, J. Sun and M. Zhao, *New J. Chem.*, 2018, **42**, 3322–3333.
- 17 J. Chao, Y. Liu, Y. Zhang, Y. Zhang, F. Huo, C. Yin, Y. Wang and L. Qin, *Spectrochim. Acta, Part A*, 2015, **146**, 33–37.
- 18 J. Chao, Y. Zhang, H. Wang, Y. Zhang, F. Huo, C. Yin, L. Qin and Y. Wang, *Sens. Actuators, B*, 2013, **188**, 200–206.
- 19 Y. Yang, F. Huo, J. Zhang, Z. Xie, J. Chao, C. Yin, H. Tong, D. Liu, S. Jin, F. Cheng and X. Yan, *Sens. Actuators, B*, 2012, **166–167**, 665–670.
- 20 H. Tian, J. Qian, Q. Sun, H. Bai and W. Zhang, *Anal. Chim. Acta*, 2013, **788**, 165–170.
- 21 M. Gómez, E. G. Perez, V. Arancibia, C. Iribarren, C. Bravo-Díaz, O. García-Beltrán and M. E. Aliaga, *Sens. Actuators, B*, 2017, **238**, 578–587.
- 22 O. García-Beltrán, C. González, E. G. Pérez, B. K. Cassels, J. G. Santos, D. Millán, N. Mena, P. Pavez and M. E. Aliaga, *J. Phys. Org. Chem.*, 2012, **25**, 946–952.
- 23 M. E. Aliaga, W. Tiznado, B. K. Cassels, M. T. Nuñez, D. Millán, E. G. Pérez, O. García-Beltrán and P. Pavez, *RSC Adv.*, 2014, **4**, 697–704.
- 24 K. Peter, T. Stefan, S. Hans-Günther and A. Andreas, *Eur. J. Org. Chem.*, 2004, 1577–1583.
- 25 O. García-Beltrán, N. Mena, O. Yañez, J. Caballero, V. Vargas, M. T. Nuñez and B. K. Cassels, *Eur. J. Med. Chem.*, 2013, **67**, 60–63.
- 26 O. García-Beltrán, N. Mena, E. G. Pérez, B. K. Cassels, M. T. Nuñez, F. Werlinger, D. Zavala, M. E. Aliaga and P. Pavez, *Tetrahedron Lett.*, 2011, **52**, 6606–6609.
- 27 J. Wang, Y. Hang, H. Tan, T. Jiang, X. Qu and J. Hua, *J. Photochem. Photobiol., A*, 2017, **346**, 265–272.
- 28 D. Jiang, H. Jiang, J. Ji, X. Sun, H. Qian, G. Zhang and L. Tang, *J. Agric. Food Chem.*, 2014, **62**, 6473–6480.
- 29 AOAC Official Method 990.28, Sulfites in Foods, Optimized Monier-Williams Method, AOAC Official Methods of Analysis, Sec. 47.3.43, 2000.
- 30 D.-P. Li, Z.-Y. Wang, J. Cui, X. Wang, J.-Y. Miao and B.-X. Zhao, *Sci. Rep.*, 2017, **7**, 45294.
- 31 G. A. Crosby and J. N. Demas, *J. Phys. Chem.*, 1971, **75**, 991–1024.

